# Apoptotic pathway induced by transduction of *RUNX3* in the human gastric carcinoma cell line MKN-1

**Yumi Nagahama,[1,6] Mika Ishimaru,[1,6] Mitsuhiko Osaki,[1,2,6,7] Toshiaki Inoue,[3] Akihiro Maeda,[4] Chisato Nakada,[4,5] Masatsugu Moriyama,[5] Kenzo Sato,[4] Mitsuo Oshimura[2] and Hisao Ito[1]**

Divisions of [1]Organ Pathology, Department of Microbiology and Pathology, Faculty of Medicine, [2]Molecular Genetics and Biofunction, Institute of Regenerative Medicine and Biofunction, [3]Human Genome Science, [4]Molecular Biology, Department of Molecular and Cellular Biology, School of Life Sciences, Faculty of Medicine Tottori University, Yonago, Tottori, 683-8503; [5]Department of Molecular Pathology, Faculty of Medicine, Oita University, Oita 879-5593, Japan

(Received August 8, 2007/Revised September 5, 2007/Accepted September 10, 2007/Online publication October 23, 2007)

**The human runt-related transcription factor 3 gene (*RUNX3*) is considered to be a candidate tumor suppressor gene in gastric carcinoma. However, the role of RUNX3 in the regulation of cell proliferation remains unclear. In the present study, we constructed an adenoviral vector encoding human *RUNX3* cDNA under the control of a Tet-responsive promoter (Ad-Tet-FLAG-RUNX3), which regulates the expression of *RUNX3* in the presence or absence of doxycycline. A recombinant adenoviral expression vector encoding *LacZ* (Ad-Tet-LacZ) was used as a negative control. The effect of the transduction of *RUNX3* on cell growth was examined using the Tet-On system in a human gastric carcinoma cell line, MKN-1. Exogenous *RUNX3* expression was induced successfully by Ad-Tet-FLAG-RUNX3, but not Ad-Tet-LacZ, in the presence of doxycycline in the MKN-1 cells. At 72 h after infection, the proliferative activity in RUNX3-expressing cells was 55% or less of that of the control cells. Flow cytometry revealed that the sub-$G_1$ peak was increased in cells expressing RUNX3 (34.11%), indicating that the inhibition of cell growth was due to apoptosis, which was confirmed based on Hoechst 33258 staining, the release of cytochrome *c* from mitochondria into the cytosol, and detection of cleaved caspase-3 by western blotting in MKN-1 cells. Comprehensive analysis using a cDNA microarray showed that RUNX3 upregulated 17 apoptosis-related genes (including *FADD*, *TRAF6*, *caspase-2*, *ING1*, *ING4*, *Calpain 10*, and *DNase1*) and downregulated 135 apoptosis-related genes (including *FLIP*, *PEA15*, *TXN2*, *HSPD1*, *IKK*, and *TIAL1*) in MKN-1 cells. Pathway analyses to generate functional networks of the genes suggested that promotion of the formation of the death-inducing signaling complex and activation of the mitochondria-mediated pathway were associated with RUNX3-induced apoptosis. In conclusion, our findings suggest that exogenous RUNX3 expression suppressed cell proliferation by inducing apoptosis via the death-receptor mitochondria-mediated pathway in MKN-1 cells. (*Cancer Sci* 2008; 99: 23–30)**

The human runt-related transcription factor 3 gene (*RUNX3*) is part of the runt-domain family of transcription factors that act as master regulators of gene expression in major developmental pathways.[1–3] *RUNX3* is a candidate tumor suppressor gene for gastric carcinoma, because the gastric mucosa in *RUNX3*$^{-/-}$ mice undergoes hyperplasia due to reduced sensitivity of gastric epithelial cells to transforming growth factor (TGF)-β growth-inhibitory activity and TGF-β-mediated apoptosis. Moreover, downregulation of RUNX3 mRNA expression, caused by the combination of a hemizygous deletion and gene silencing due to hypermethylation of the promoter region, occurs in human gastric carcinoma cell lines and primary carcinoma tissues.[4–9] Furthermore, it has been reported that RUNX3 mRNA expression is downregulated in human colon,[8] bile duct,[10] pancreatic,[10] lung,[11] and hepatocellular[12–14] carcinoma cell lines. Although it is well established that RUNX3 is a transcription factor, only a small number of the genes targeted by RUNX3, including *Bim*,[15] are known so far, and many other details remain to be elucidated.

Adenoviral vectors are powerful vehicles for the transfer of genes into epithelial and carcinoma cells. However, the transduction of a gene by an adenoviral vector can not be regulated specifically. Control of the transgene's expression is essential for analyzing gene function. The Tet-On system provides several advantages over other systems for controlling the expression of transgenes. For example, it has precise regulation, high inducibility, quick response, and no pleiotrophic effect due to the use of a tetracycline (Tet) operon derived from bacteria and a well-characterized inducer: Tet or doxycycline (Dox), a Tet analog.[16,17] In the Tet-On system, the reverse Tet-responsive transcriptional activator, which was created by four amino acid changes in the Tet repressor protein, binds to the Tet-responsive element, and turns on transcription in the presence of Tet or Dox.[17] Therefore, it is thought that the signaling pathway triggered by RUNX3 will be disclosed clearly by using the Tet-On system.

In the present study, we constructed a Tet-responsive adenoviral vector encoding FLAG-tagged RUNX3 cDNA (Ad-Tet-FLAG-RUNX3), which conditionally expresses RUNX3, to examine: (i) the role of RUNX3 in the inhibition of cell growth; and (ii) the gene expression pattern with a DNA microarray to identify the genes whose expression is increased or decreased by RUNX3 in human gastric carcinoma cells.

## Materials and Methods

**Construction of the adenoviral vector.** FLAG-tagged RUNX3 cDNA was generated by polymerase chain reaction (PCR) using pEFBOS/RUNX3 (kindly provided by Professor Yoshiaki Ito, National University of Singapore) as a template and a primer pair: 5′-TTGCTAGCACCATGGACTACAAAGACGACGATGACG-ACAAGCGTATTCCCGTAGAGACCCA-3′ and 5′-TTGCGG-CTCAGTAGGGCCGCCACAC-3′. The PCR fragment was subcloned into the pT7Blue T-Vector (Novagen, Darmstadt, Germany). Sequencing was carried out to confirm the identity and orientation of the FLAG-tagged *RUNX3* gene in this construct. The FLAG-RUNX3 fragment was excised by *Nhe*I and *Not*I from pT7Blue T-Vector/FLAG-RUNX3. This fragment was ligated into the same site of pIRES-hrGFP-1a (Stratagene, La Jolla, CA,

[6]These authors contributed equally to this work.
[7]To whom correspondence should be addressed.
E-mail: osamitsu@grape.med.tottori-u.ac.jp

doi: 10.1111/j.1349-7006.2007.00650.x

USA). A Tet-regulated adenoviral vector encoding FLAG-RUNX3 (Ad-Tet-FLAG-RUNX3) was constructed using the BD Adeno-X Tet-On Expression system 1 (Takara Bio, Otsu, Japan). The construction of Ad-Tet-FLAG-RUNX3 was achieved according to the manufacturer's instructions. The generated virus was purified by sequential centrifugation in CsCl step gradients.[18] The titer of virus was determined using an Adeno-X rapid titer kit (Takara Bio) following the manufacturer's directions. An adenoviral vector encoding a reverse Tet repressor (Ad-Tet-On), and a Tet-regulated adenoviral vector encoding *LacZ* (Ad-Tet-LacZ), which was used as a control vector, were also constructed and purified as well as Ad-Tet-FLAG-RUNX3.

**Cell line and conditions for adenovirus-mediated transduction.** MKN-1, a human gastric carcinoma cell line, was used in the present study because higher efficiency of gene transduction via adenovirus vector was reported in MKN-1,[19] although MKN-1 showed RUNX3 expression as described previously.[20] The cells were cultured in Dulbecco's modified Eagle's medium (DMEM) supplemented with 10% fetal bovine serum and antibiotics in a 5% $CO_2$ incubator at 37°C. They were co-infected with Ad-Tet-On and either Ad-Tet-LacZ or Ad-Tet-FLAG-RUNX3 at a multiplicity of infection (MOI) of 40 (Ad-Tet-On, MOI 20; Ad-Tet-LacZ or Ad-Tet-FLAG-RUNX3, MOI 20) for western blotting, flow cytometry, and immunocytochemistry, and a MOI of 60 (Ad-Tet-On, MOI 30; Ad-Tet-Lac or Ad-Tet-FLAG-RUNX3, MOI 30) for assessing cell viability. Dox (1 μg/mL, final concentration) was added at 1 and 48 h after the introduction of these adenoviral vectors.

**Western blotting.** At 0, 24, 48, and 72 h after infection, the cells were washed twice with phosphate-buffered saline (PBS) (–), harvested, and solubilized in lysis buffer (20 mM Tris-HCl [pH 7.4], 150 mM NaCl, 0.1% sodium dodecylsulfate, 1% sodium deoxycholate, 1% Triton X-100, 1 mM phenylmethylsulfonyl fluoride (PMSF), 5 mg/mL aprotinin, and 1 μg/mL leupeptin). Equal amounts of protein were separated by electrophoresis on sodium dodecylsulfate–polyacrylamide gels, electrotransferred to a polyvinylidene difluoride filter (Millipore, Bedford, MA, USA), then blotted with anti-FLAG monoclonal antibody (mAb) (M2, 10 μg/mL; Sigma, St Louis, MO, USA). Blots were developed with peroxidase-labeled antimouse or antirabbit antibodies (1:2000; MBL, Nagoya, Japan) using enhanced chemiluminescence (ECL detection system; Amersham, Buckinghamshire, UK).

**Immunocytochemistry.** MKN-1 cells were seeded at $6 \times 10^4$ cells per well in six-well plates on which glass coverslips were placed. At 24 h after infection, the cells were fixed in 4% formaldehyde for 10 min at 4°C. Immunocytochemistry was carried out using the streptavidin–peroxidase complex (SAB) method with a Histofine SAB-PO (M) immunohistochemical staining kit (Nichirei, Tokyo, Japan). Mouse monoclonal antibody against FLAG (M2, 20 μg/mL; Sigma) and rabbit polyclonal antibody against RUNX3[20] were used as primary antibodies. Immunoreactions were visualized with diaminobenzidine, and the cells were counterstained with hematoxylin.

**Cell viability.** Cells were plated at a density of $2 \times 10^3$ cells/well in 96-well plates. After incubation overnight, cells were co-infected with Ad-Tet-On and Ad-Tet-LacZ or Ad-Tet-FLAG-RUNX3 at a MOI of 60 (Ad-Tet-On, MOI 30; Ad-Tet-LacZ or Ad-Tet-FLAG-RUNX3, MOI 30) and Dox was added to each well at a final concentration of 1 μg/mL, 1 and 48 h after the infection. Cell viability was assessed using the 3-(4,5-dimethylthiazol-2-yl)-2,5-diphenyltetrazolium bromide (MTT) assay (Dojindo, Kumamoto, Japan) according to the manufacturer's instructions.

**Evaluation of apoptosis.** At 48 or 72 h after infection, the cells, either infected with Ad-Tet-FLAG-RUNX3 or Ad-Tet-LacZ, or else not infected, were evaluated for apoptosis using three different methods.

(1) Flow cytometry: Cells were trypsinized, washed twice with PBS (–), fixed in 70% ethanol, treated with RNase (250 μg/mL), and stained with propidium iodide. A flow cytometer (Epics XL; Coulter, Hialeah, FL, USA) was then used to analyze their DNA content.
(2) Hoechst 33258 staining: Cells were trypsinized, washed twice with PBS (–), fixed with Clarke's fixative (ethanol : acetic acid = 3:1), and allowed to dry in air. They were then stained with 1 mg/mL Hoechst 33258 for 10 min in the dark at room temperature. After staining, the cells were washed three times with distilled water for 5 min. Coverslips were mounted onto slides and apoptotic bodies were visualized using an ultraviolet laser microscope.
(3) Detection of cytochrome *c* release and cleaved caspase-3: Cells were harvested and mitochondrial and cytosolic fractions were separated using a Mitochondria/Cytosol Fractionation Kit (BioVision, Lyon, France) according to the instructions of the manufacturer. The extraction of whole cell lysate and western blotting were carried out as described above. An antihuman cytochrome *c* mAb (7H8.2C12, 1:500; BD Biosciences, San Jose, CA, USA), anticleaved caspase-3 polyclonal antibody (1:500; Cell Signaling, Beverly, MA, USA), and anti-β-actin mAb (AC-15, 1:2000; Sigma) were used.

**Statistical analysis.** The statistical analysis was carried out with an analysis of variance (ANOVA). A *P*-value of less than 0.05% was considered to indicate significance.

**cDNA microarray, pathway analyses, and reverse transcription-PCR.** MKN-1 cells were plated at a density of $3 \times 10^5$ cells per 100 mm-diameter dish. After incubation overnight, the cells were co-infected with Ad-Tet-On and Ad-Tet-LacZ or Ad-Tet-FLAG-RUNX3 at a MOI of 40 (Ad-Tet-On, MOI20; Ad-Tet-LacZ or Ad-Tet-FLAG-RUNX3, MOI20) and 1 μg/mL Dox was added at 1 h after the infection. After 24 h of treatment, the cells were harvested to extract total RNA using an RNAeasy kit (Qiagen, Valencia, CA, USA). The total RNA was treated using DNase to eliminate any contaminating DNA. The integrity of the RNA was checked by electrophoresis on a 1% formaldehyde gel. From 5 μg of total RNA, RNA probes were generated using a MessageAmp RNA kit (Ambion, Austin, TX, USA). For transcriptomic profiling, we used an oligonucleotide-based DNA microarray, AceGene Human Oligo Chip 30K (DNA Chip Research, Yokohama, Japan). Hybridizations and washes were carried out by following the directions recommended by the manufacturer. Scanning of the microarray was carried out using a Fuji FLA-8000 Scanner (FUJIFILM Life Science, Tokyo, Japan). The intensity of each hybridized cDNA was evaluated using Array Gauge Software (FUJIFILM Life Science) and the Cye5/Cye3 ratio for each gene was calculated. A Cye5/Cye3 ratio greater than or equal to 2.00, or less than or equal to 0.50 was used to define whether the expression of a gene was upregulated or downregulated, respectively. The genes selected according to this definition were uploaded into the Ingenuity Pathways Analysis suite in order to identify apoptosis-related networks of interacting genes (http://www.ingenuity.com). To confirm the relative expression detected by DNA microarray and pathway analyses, reverse transcription (RT)-PCR was carried out for six genes (*TRAF6*, *HSPA5*, *TXN2*, *HSPD1*, *PEA15*, and β-*actin*). Total RNA was isolated as described above and cDNA was synthesized as a conventional method. The sequences of primers were 5′-gtcctctaccagcgccttg-3′ and 5′-tccacagctgttttcacagttt-3′ for *TRAF6*, 5′-catcaagttcttgccgttca-3′ and 5′-tcttcaggagcaaatgtctttgt-3′ for *HSPA5*, 5′-gtggatttccacgcacagt-3′ and 5′-atatccaccttggccatcac-3′ for *TXN2*, 5′-cctgcactctgtccctcact-3′ and 5′-ggtaaccgaagcatttctgc-3′ for *HSPD1*, 5′-gagaataaggagcctttcttatgga-3′ and 5′-tctgctgaaaag-aaccctgtc-3′ for *PEA15*, and 5′-ccaaccgcgagaagatga-3′ and 5′-ccagaggcgtacagggatag-3′ for β-actin, and 30 cycles of PCR were carried out. The annealing temperature was at 59°C and PCR products were confirmed by 12% polyacrylamide gel electrophoresis, followed by ethidium bromide staining.


doi: 10.1111/j.1349-7006.2007.00650.x

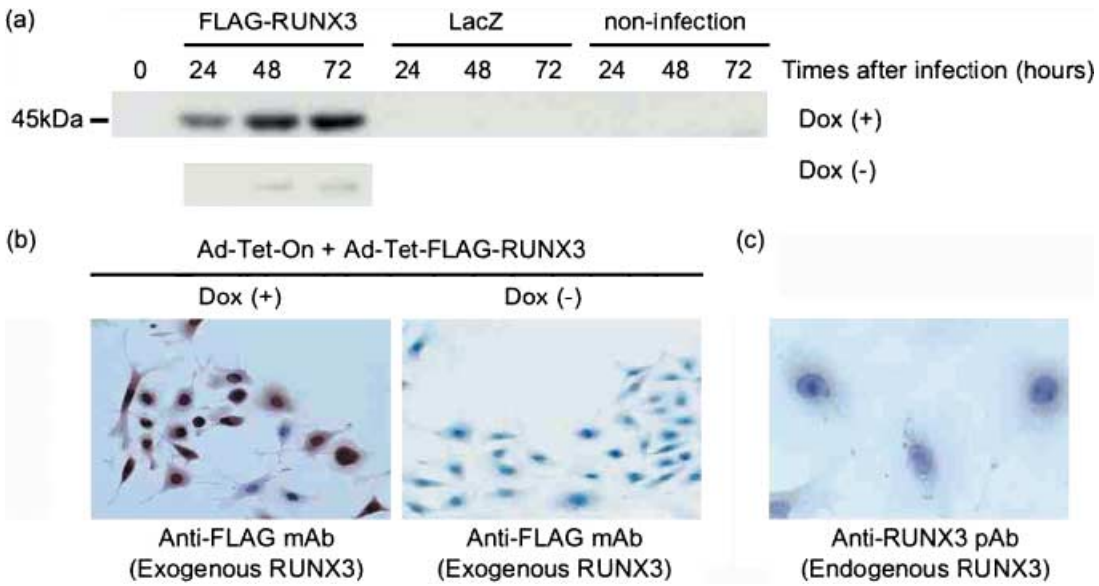


**Fig. 1.** Doxycycline (Dox)-regulated runt-related transcription factor 3 (RUNX3) expression. (a) Western blot analysis of RUNX3 expression in MKN-1 cells. The MKN-1 cells were co-infected at a multiplicity of infection (MOI) of 40 (Ad-Tet-On, MOI 20; Ad-Tet-LacZ or Ad-Tet-FLAG-RUNX3, MOI 20) or left uninfected and cultured with or without Dox (1 μg/mL). At the indicated time points, the cells were harvested and subjected to western blotting with anti-FLAG antibody. (b) Immunocytochemical detection of FLAG-RUNX3 in MKN-1 cells co-infected with Ad-Tet-On and Ad-Tet-FLAG-RUNX3. MKN-1 cells were seeded at $6 \times 10^4$ cells per six-well plate. At 24 h after co-infection at a MOI of 40 (Ad-Tet-On, MOI 20; Ad-Tet-FLAG-RUNX3, MOI 20), immunocytochemistry was carried out. (c) Immunocytochemical detection of endogenous RUNX3 in MKN-1 cells using anti-RUNX3 polyclonal antibody. Immunoreactivity was observed only in the cytoplasm.

## Results

**Tet-regulated expression of RUNX3.** Western blotting was carried out to examine the expression of exogenous RUNX3 by the Tet-On system. The expression was detected at least 24 h after infection with Ad-Tet-FLAG-RUNX3 and Ad-Tet-On, but not Ad-Tet-LacZ or no infection, and the expression level was maintained at least until 72 h in the presence, but not absence, of Dox (Fig. 1a).

Then, we carried out immunocytochemistry using mouse anti-FLAG antibody to examine the efficiency and localization of RUNX3 expression in MKN-1 cells. As shown in Fig. 1b, when co-infected with Ad-Tet-On and Ad-Tet-FLAG-RUNX3, most MKN-1 cells showed RUNX3 (FLAG) immunoreactivity with the Dox treatment, whereas none of the cells did so without the Dox treatment at 24 h after infection, the immunoreactivity being detected in both the nucleus and cytoplasm in the former (Fig. 1b). Although endogenous RUNX3 expression in MKN-1 was also detected, immunoreactivity for RUNX3 was observed only in the cytoplasm (Fig. 1c). These results suggest that RUNX3 was significantly transduced in the presence of Dox compared to the absence of Dox in MKN-1 cells co-infected with Ad-Tet-On and Ad-Tet-FLAG-RUNX3, and that exogenous overexpressed functional RUNX3 protein was translocated into the nucleus.

**Inhibition of cell proliferation by enforced expression of RUNX3 in MKN-1 cells.** A MTT assay was carried out to examine whether enforced expression of RUNX3 could suppress cell proliferation. The viability of the cells demonstrated significant inhibition of proliferation in MKN-1 cells transduced with RUNX3 in a time-dependent manner, compared to LacZ-transduced or non-transduced cells (Fig. 2a; $P < 0.001$). MKN-1 cells co-infected with Ad-Tet-On and Ad-Tet-LacZ or non-infected cells did not show growth inhibition even in the presence of Dox (Fig. 2a). In the case without Dox treatment, the growth rate of RUNX3-transduced cells did not differ significantly from that of LacZ-transduced or non-transduced cells as controls (Fig. 2b). These results suggest that *RUNX3* acted as a suppressor of cell proliferation in MKN-1.

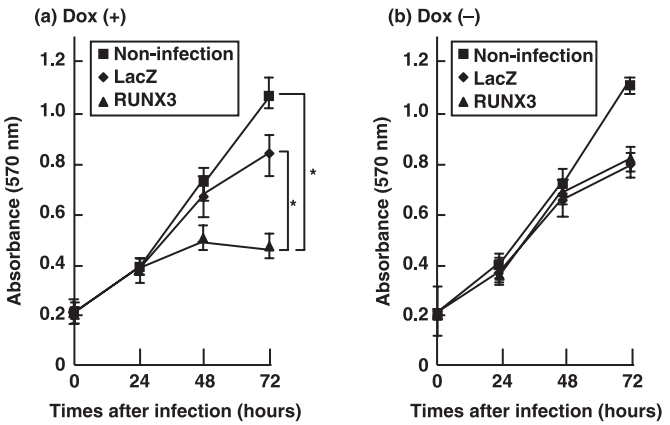


**Fig. 2.** Growth inhibition by runt-related transcription factor 3 (RUNX3) as determined using the MTT assay. MKN-1 cells were infected at a multiplicity of infection (MOI) of 60 (Ad-Tet-On, MOI 30; Ad-Tet-LacZ or Ad-Tet-FLAG-RUNX3, MOI 30) or left uninfected, and incubated (a) in the presence of doxycycline (Dox) (1 μg/mL), or (b) in the absence of Dox. Values for the Ad-Tet-FLAG-RUNX3 group are significantly suppressed compared to those for the Ad-Tet-LacZ or uninfected groups in a time-dependent manner. *$P < 0.0001$ FLAG-RUNX3 versus LacZ, or no infection. Values are means of two quadruplicate studies for each group ± SD.

Flow cytometry revealed that the percentage of cells with a sub-$G_1$ peak, indicative of apoptosis, was as high as 34.11%, compared with 7.05% in LacZ-transduced cells. The cell percentage in $G_0/G_1$ phase, S phase, and $G_2/M$ phase was 31.91, 10.45, and 23.53% in the RUNX3-transduced cells, and 48.07, 8.66 and 36.22% in the LacZ-transduced cells, respectively (Fig. 3a). These data indicated that apoptosis was induced by enforced expression of RUNX3 in the MKN-1 cells. Then,

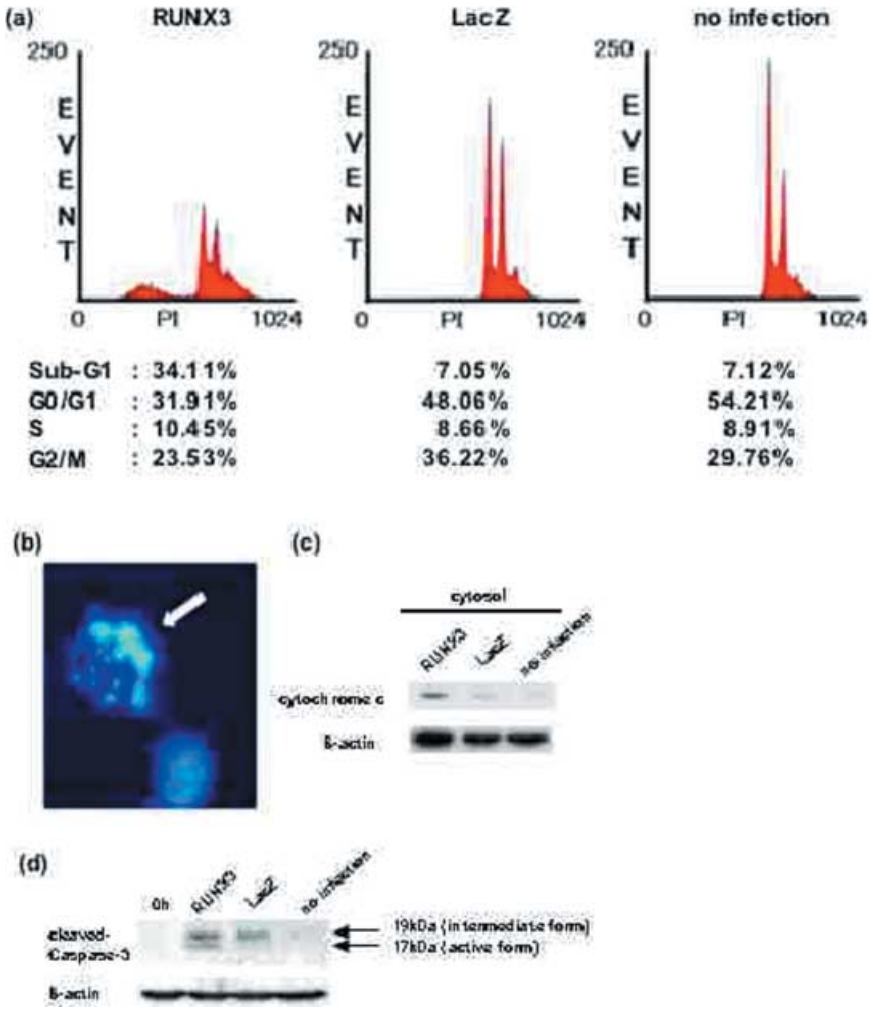


**Fig. 3.** Detection of apoptotic cells. MKN-1 cells were co-infected at a multiplicity of infection (MOI) of 40 (Ad-Tet-On, MOI 20; Ad-Tet-LacZ or Ad-Tet-FLAG-RUNX3, MOI 20) or left uninfected, and cultured with doxycycline (Dox) (1 μg/mL). (a) Detection of apoptotic cells by flow cytometry. After 72 h, cells were centrifuged and fixed in 70% ethanol. Samples were then treated with RNase, stained with propium iodide, and analyzed by flow cytometry. A sub-$G_1$ peak was clearly detected when runt-related transcription factor 3 (RUNX3) was transduced in MKN-1 cells (left panel). (b) Morphological examination to detect apoptosis by Hoechst 33258 staining. At 72 h after infection, cells were stained with Hoechst 33258. MKN-1 cells transduced with RUNX3 underwent several morphological changes, including chromatin margination, nuclear condensation, and fragmentation, which are characteristic of apoptosis. Photomicrographs were taken with an ultraviolet laser microscope at ×600 magnification. (c,d) Detection of cytochrome *c* release and cleaved caspase-3 protein. MKN-1 cells were co-infected at a MOI of 40 (Ad-Tet-On, MOI 20; Ad-Tet-LacZ or Ad-Tet-FLAG-RUNX3, MOI 20) or left uninfected, and cultured with Dox (1 μg/mL). At 48 h after the infection, the cytosolic fraction or whole-cell fraction was extracted to determine the expression level of cytochrome *c* and cleaved caspase-3 protein by western blotting, respectively. β-Actin was used as an internal control.

apoptosis was also confirmed morphologically by Hoechst 33258 staining by RUNX3 expression in MKN-1 (Fig. 3b). In addition, cytochrome *c* release from the mitochondria into the cytosolic fraction and appearance of cleaved caspase-3 was observed in RUNX3-transduced cells (Fig. 3c,d). These results suggest that enforced expression of RUNX3 inhibited cell proliferation by inducing apoptosis via a mitochondria-mediated pathway in MKN-1 cells.

**Profiling of RUNX3-responsive apoptosis-related genes using cDNA microarrays.** In order to obtain further insights into the molecular mechanisms underlying the apoptosis induced by RUNX3 expression, we compared LacZ- and RUNX3-transduced MKN-1 cells for 24 h for their apoptosis-related gene expression profiles, using cDNA microarrays (AceGene Human Oligo Chip 30K) encompassing approximately 30 000 genes. A list of all genes analyzed using the cDNA microarray is shown in Suppl. Table 1. In Tables 1 and 2, a total of 152 apoptosis-related genes were identified as being differentially expressed between LacZ- and RUNX3-transduced cells, among which 17 were upregulated and 135 were downregulated in response to overexpression of RUNX3. Interestingly, the levels of many caspase family members were elevated, although these expression ratios compared to Ad-Tet-LacZ were less than 2.00 (i.e. 1.42/caspase-1, 1.32/caspase-3, 1.19/caspase-7, 1.57/caspase-8, and 1.09/caspase-10, respectively), except for caspase-2 (3.017).

The identified genes were subjected to an ingenuity pathways analysis to generate functional networks of apoptosis-related genes responding to RUNX3 expression in the MKN-1 cells. As shown in Fig. 4, RUNX3 probably activates the death-receptor mitochondria-mediated apoptotic pathway in MKN-1. In addition, RT-PCR data of the six genes were consistent with cDNA microarray data (Fig. 5).

**Table 1. Greater than 2.0-fold upregulated apoptosis-related genes in MKN-1 cells infected with Ad-Tet-FLAG-RUNX3**

| Gene name | Accession no. | Ratio† |
|---|---|---|
| *C21orf107* | NM_033656 | 4.973 |
| *FADD* | BC000334 | 4.679 |
| *PIK3R3* | NM_003629 | 4.192 |
| *DNASE1* | AC005203 | 4.057 |
| *CD5L* | NM_005894 | 3.901 |
| *CASP2* | BC002427 | 3.017 |
| *TRAF6* | NM_004620 | 3.129 |
| *PRKCL1* | NM_002741 | 2.806 |
| *KIAA0971* | NM_014929 | 2.662 |
| *RASA1* | NM_002890 | 2.418 |
| *CAPN10* | AF089090 | 2.375 |
| *GIP3* | NM_022873 | 2.320 |
| *WWOX* | U13395 | 2.203 |
| *ING1* | AB037594 | 2.196 |
| *PLA2G6* | NM_003560 | 2.151 |
| *ING4* | NM_016162 | 2.151 |
| *GZMB* | NM_004131 | 2.025 |

†Cy5/Cy3 ratio.


doi: 10.1111/j.1349-7006.2007.00650.x

**Table 2. Less than 0.5-fold downregulated apoptosis-related genes in MKN-1 cells infected with Ad-Tet-FLAG-RUNX3**

| Gene name | Accession no. | Ratio† | Gene name | Accession no. | Ratio† | Gene name | Accession no. | Ratio† | Gene name | Accession no. | Ratio† |
|---|---|---|---|---|---|---|---|---|---|---|---|
| *WDR6* | AK022719 | 0.495 | *CAD* | AB028911 | 0.426 | *APOE* | NM_000041 | 0.361 | *VEGF* | NM_003376 | 0.284 |
| *IL18* | NM_001562 | 0.494 | *TNFAIP3* | NM_006290 | 0.425 | *VHL* | NM_000551 | 0.358 | *WWOX* | AF395124 | 0.278 |
| *ATM* | NM_000051 | 0.494 | *ENC1* | NM_003633 | 0.423 | *PML* | AF230401 | 0.358 | *ADRA1A* | AF013261 | 0.277 |
| *PRSS25* | AF141307 | 0.486 | *CLDN3* | AB000714 | 0.423 | *GPR65* | NM_003608 | 0.358 | *IL2RA* | NM_000417 | 0.275 |
| *HIP1* | NM_005338 | 0.486 | *NME4* | NM_005009 | 0.423 | *RNF7* | AF312226 | 0.357 | *HSPA5* | AF188611 | 0.274 |
| *SULF1* | AL136772 | 0.484 | *YARS* | BC001933 | 0.423 | *IFNB1* | NM_002176 | 0.352 | *ELKS* | AB015617 | 0.273 |
| *CAPN1* | NM_005186 | 0.481 | *TNFRSF9* | NM_001561 | 0.422 | *CASP8AP2* | NM_012115 | 0.351 | *TDGF1* | NM_003212 | 0.270 |
| *THY1* | NM_006288 | 0.478 | *WDR26* | NM_025160 | 0.420 | *YWHAH* | NM_003405 | 0.349 | *ELKS* | AK000148 | 0.268 |
| *TRADD* | NM_003789 | 0.475 | *TXN2* | NM_012473 | 0.420 | *BIRC5* | BC000784 | 0.347 | *PEA15* | BC010469 | 0.267 |
| *IRAK2* | NM_001570 | 0.471 | *TIAL1* | NM_022333 | 0.417 | *BCL2L14* | AF281254 | 0.346 | *C20orf109* | AL118499 | 0.264 |
| *C20orf35* | NM_018478 | 0.470 | *MYBL2* | NM_002466 | 0.416 | *DNAJA3* | NM_005147 | 0.346 | *TNFRSF14* | NM_003820 | 0.263 |
| *PAX7* | NM_013945 | 0.470 | *CDKN2A* | S78535 | 0.416 | *ARHGEF6* | D25304 | 0.345 | *TIMP3* | NM_000362 | 0.259 |
| *OLR1* | NM_002543 | 0.463 | *INHA* | NM_002191 | 0.413 | *SIVA* | NM_006427 | 0.343 | *HSPD1* | NM_002156 | 0.257 |
| *KIAA0982* | NM_014023 | 0.461 | *CASP14* | NM_012114 | 0.406 | *PRKAR2A* | NM_004157 | 0.341 | *VDAC1* | NM_003374 | 0.255 |
| *CDC2L5* | BC001274 | 0.461 | *TPD52L1* | NM_003287 | 0.403 | *IL1B* | NM_000576 | 0.335 | *NRG2* | NM_013981 | 0.251 |
| *IL3* | NM_000588 | 0.458 | *ADRA1A* | NM_000680 | 0.403 | *RBMS1* | NM_016836 | 0.331 | *SON* | X63753 | 0.249 |
| *MAEA* | AK022515 | 0.458 | *IL2* | NM_000586 | 0.403 | *IL2RB* | NM_000878 | 0.323 | *BIK* | NM_001197 | 0.249 |
| *NID2* | NM_007361 | 0.457 | *PDCL3* | NM_024065 | 0.402 | *PAK2* | NM_002577 | 0.323 | *STK4* | NM_006282 | 0.248 |
| *NOX5* | NM_024505 | 0.457 | *EBAG9* | NM_004215 | 0.399 | *PIK3R1* | U49349 | 0.323 | *SART1* | NM_005146 | 0.236 |
| *MAL* | NM_022438 | 0.454 | *IKK* | AF009225 | 0.398 | *CD74* | ENSG00000019582 | 0.321 | *PAX3* | U12259 | 0.228 |
| *GAB1* | NM_002039 | 0.452 | *DEDD* | AJ010973 | 0.397 | *IRAK4* | NM_016123 | 0.321 | *TRAF2* | NM_021138 | 0.225 |
| *NMT1* | NM_021079 | 0.451 | *NIK* | NM_003954 | 0.397 | *NALP2* | NM_017852 | 0.319 | *CUL1* | NM_003592 | 0.224 |
| *CARD15* | NM_022162 | 0.450 | *CLC* | NM_013246 | 0.391 | *CUGBP2* | NM_006561 | 0.319 | *BCAP31* | NM_005745 | 0.224 |
| *FKSG2* | NM_021631 | 0.445 | *SERPINB9* | NM_004155 | 0.390 | *CAPNS1* | NM_001749 | 0.317 | *CLK2* | NM_003993 | 0.222 |
| *PDIP* | NM_006849 | 0.444 | *MAPK9* | NM_002752 | 0.383 | *BCL2L13* | AF183411 | 0.311 | *AKT2* | NM_001626 | 0.222 |
| *IL6* | NM_000600 | 0.442 | *PTK2B* | NM_004103 | 0.383 | *FLIP* | NM_003879 | 0.303 | *TNFRSF11B* | NM_002546 | 0.209 |
| *MGC16063* | BC008044 | 0.442 | *HTATIP2* | BC002439 | 0.378 | *CDKN1A* | NM_078467 | 0.302 | *PIK3C2B* | NM_002646 | 0.198 |
| *C22orf3* | NM_012265 | 0.441 | *NUDT2* | U30313 | 0.372 | *NALP1* | NM_033004 | 0.299 | *CASP4* | NM_001225 | 0.195 |
| *WDR5* | BC001635 | 0.439 | *IL1R1* | NM_000877 | 0.372 | *S100B* | NM_006272 | 0.299 | *SLC25A6* | AY007135 | 0.166 |
| *ELMO3* | NM_024712 | 0.437 | *TNFSF6* | NM_000639 | 0.371 | *ARHB* | NM_004040 | 0.292 | *MAEA* | AF084928 | 0.163 |
| *ITGB2* | NM_000211 | 0.437 | *CFL1* | NM_005507 | 0.368 | *RAD21* | NM_006265 | 0.291 | *CSF2RB* | NM_000395 | 0.161 |
| *TNFSF5* | NM_000074 | 0.433 | *ALB* | AF190168 | 0.366 | *IAPP* | NM_000415 | 0.287 | *PDCD6IP* | AF151793 | 0.158 |
| *HSXIAPAF1* | NM_017523 | 0.433 | *PAX3* | NM_000438 | 0.364 | *PHF17* | NM_024900 | 0.285 | *GRID2* | NM_001510 | 0.158 |
| *ACINUS* | AF124728 | 0.432 | *CD3G* | NM_000073 | 0.363 | *IL1RAP* | AB006537 | 0.285 | | | |

†Cy5/Cy3 ratio.

## Discussion

In the present study, immunoreactivity was detected in both the nucleus and cytoplasm in RUNX3-transduced MKN-1 cells, but it was not detected in the absence of Dox. In addition, endogenous expression of RUNX3 was observed in the cytoplasm but not in the nucleus in MKN-1 cells. Ito *et al*. previously demonstrated that RUNX3 was inactivated in MKN-1 cells via cytoplasmic retention of the protein.[21] Taken together, these results suggest that RUNX3 is transferred from the cytoplasm to the nucleus to exert its function as a transcription factor.

Enforced expression of RUNX3 inhibited proliferation of MKN-1 cells by inducing apoptosis, which was confirmed by flow cytometry, Hoechst 33258 staining, and cytochrome *c* release. Recently, Wei *et al*. reported that RUNX3 expression using an adenoviral vector inhibited proliferation of the gastric carcinoma cell lines N81-7 (mutated-type p53) and AGS (wild-type p53).[22] They showed that RUNX3 induced cell-cycle arrest at $G_1$ in N81-7 or apoptosis in AGS, whereas we confirmed that RUNX3 expression induced apoptosis in MKN-1 (mutated-type p53). These results suggest that RUNX3 had a critical role in inducing apoptosis or $G_1$ arrest in a cell-type dependent manner, and apoptosis induction by RUNX3 might occur in a p53-independent manner.

Although RUNX3 has been known to cause apoptosis in gastric epithelial cells and carcinoma cells,[4,15] its role in cell death signaling is not completely understood. To disclose the apoptotic signaling pathway activated by RUNX3 in MKN-1, we used a cDNA microarray to identify apoptosis-related genes comprehensively. Enforced expression of RUNX3 activated the transcription of a number of genes, including those for Fas-associated death domain (FADD), GZMB, TRAF6, DNASE1, CASP2, ING4, ING1, FLICE/caspase-8-inhibitory protein (FLIP), PEA15, and TIAL1, which play a pivotal role in the regulation of apoptosis. FADD is a member of the death-inducing signaling complex (DISC),[23] and participates in the death signaling initiated by Fas/CD95, tumor necrosis factor receptor I, death receptor 3, and death receptor 4/5.[24] In contrast, FLIP inhibits the formation of DISC by competing with caspase-8 for binding to FADD.[25] Of interest, the cDNA microarray data showed that RUNX3 expression upregulated FADD and downregulated FLIP. These results suggest that susceptibility to death receptor-mediated apoptosis might be enhanced by RUNX3 expression in MKN-1 cells.

Scaffidi *et al*. have reported that death-receptor acts via two main pathways of apoptosis in mammalian cells:[26] (i) the death-receptor pathway, directly activating caspase-3 (type I);[27] and (ii) the mitochondrial pathway, regulated by the Bcl-2 family (type II).[28] We previously reported that anti-Fas antibody induces apoptosis through the type II signaling pathway in

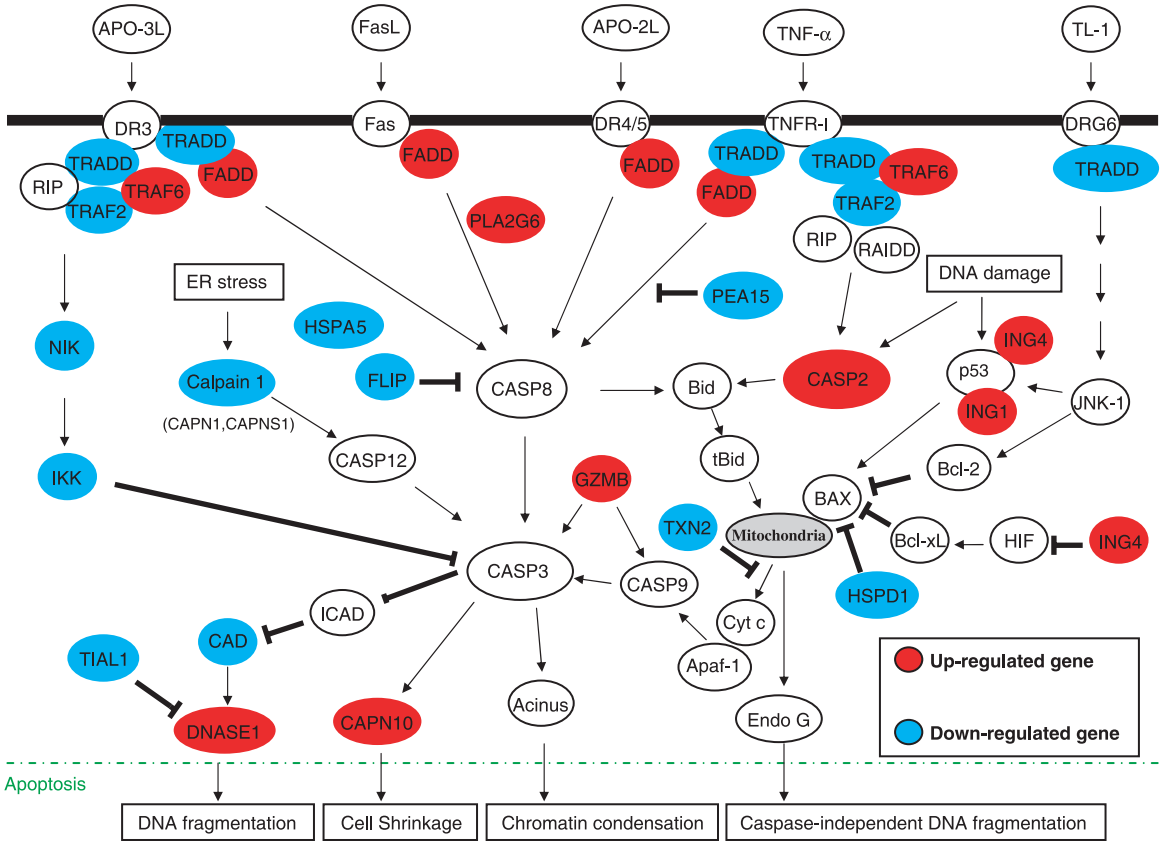


**Fig. 4.** A hypothetical schematic representation of the signaling pathways leading to apoptosis in response to the overexpression of runt-related transcription factor 3 (RUNX3) in MKN-1 cells. Upregulated and downregulated genes are indicated in red and blue, respectively. Many molecules whose expression was altered by enforced expression of RUNX3 are associated with the death-inducing signaling complex or the regulation of cytochrome *c* release from mitochondria.

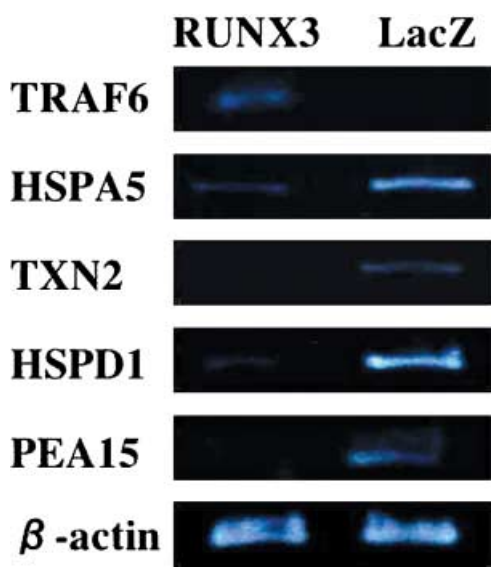


**Fig. 5.** Reverse transcription–polymerase chain reaction analysis of the *TRAF6*, *HSPA5*, *TXN2*, *HSPD1*, *PEA15*, and β-*actin* genes. RUNX3, Ad-Tet-FLAG-RUNX3-infected MKN-1 cells; LacZ, Ad-Tet-LacZ-infected MKN-1 cells.

human gastric carcinoma cells.[29] In fact, the release of cytochrome *c* from mitochondria was observed when RUNX3 was overexpressed in MKN-1 cells. Additionally, the cDNA microarray data showed upregulation of ING1 and ING4, which promote mitochondria-mediated apoptosis via the activation of p53 or suppression of hypoxia inducible factor,[30–32] and downregulation of TXN2 and HSPD1, which suppress cytochrome *c* release from the mitochondria,[33,34] caused by RUNX3 expression in the MKN-1 cells. These findings suggest that RUNX3 induced apoptosis through the mitochondria-mediated pathway by regulating the transcription of those genes. It is well established that the released cytochrome *c* forms a complex with Apaf-1 and caspase-9 (apoptosome),[35] which is followed by caspase-3 activation. Western blotting also revealed that the expression of RUNX3 activated caspase-3, following activation of DNaseI and probably calpain-10,[36,37] which induces DNA fragmentation and cell shrinkage, typical morphological features of apoptosis.

Wei *et al*. reported that enforced expression of RUNX3 by an adenoviral vector led to the expression of caspase-3, -7, and -8 mRNA in AGS cells.[22] In our study, RUNX3 transduction by Ad-Tet-FLAG-RUNX3 also upregulated caspase-3, -7, and -8 mRNA expression in MKN-1 cells, although the expression ratio compared to Ad-Tet-LacZ was less than 2.00 (i.e. 1.32/caspase-3, 1.19/caspase-7, and 1.57/caspase-8). In addition, Peng *et al*. showed that *RUNX3* gene transfer suppressed vascular endothelial growth factor (VEGF) expression in two human gastric cancer cell lines, NCI-N87 and SK-GT5.[38] Our results also showed that enforced expression of RUNX3 downregulated the expression of VEGF mRNA. These findings indicate that various molecules might be commonly regulated by RUNX3 expression in a variety of human gastric cancer cell lines, and support the reliability of our cDNA microarray data. However, Yamamura *et al*. showed that RUNX3 cooperates with FoxO3a/FKHRL1, forkhead transcription factor, to induce apoptosis of


doi: 10.1111/j.1349-7006.2007.00650.x

AGS cells by upregulation of Bim,[15] which is a BH3-only protein and acts as a pro-apoptotic factor.[39] Our study, however, did not demonstrate the upregulation of Bim expression in RUNX3-transduced MKN-1 cells. It is also suggested that the molecules regulated by RUNX3 might differ in a cell-type dependent manner.

In summary, we constructed an adenoviral vector encoding human RUNX3 cDNA under the control of the Tet-responsive promoter (Ad-Tet-FLAG-RUNX3), which is an attractive strategy for the analysis of gene function. Enforced RUNX3 expression using Ad-Tet-FLAG-RUNX3 showed growth inhibition and apoptosis induced probably via the death-receptor mitochondria-mediated pathway in MKN-1 cells. Moreover, the present findings might aid in the design of effective therapeutic treatments for human gastric carcinoma.

## Acknowledgments

We thank Professor Yoshiaki Ito (Institute of Molecular and Cell Biology, The National University of Singapore) for kindly providing human *RUNX3* cDNA. We also thank Mr Masato Isono and Ms Momoe Itsumi for their excellent technical advice. This work was supported, in part, by Grants-in-Aid for Scientific Research from the Ministry of Education, Culture, Sports, Science, and Technology of Japan (grant numbers 14370069 and 16790207).

## References

1 Leavanon D, Bernstein Y, Negreanu V *et al*. A large variety of alternatively spliced and differentially expressed mRNAs are encoded by the human acute myeloid leukemia gene *AML1*. *DNA Cell Biol* 1996; **15**: 175–85.
2 Ito Y. Molecular basis of tissue-specific gene expression mediated by the runt domain transcription factor PEBP/CBF. *Gene Cells* 1999; **4**: 685–96.
3 Bangsow C, Rubins N, Glusman G *et al*. The *RUNX3* gene-sequence, structure and regulated expression. *Gene* 2001; **279**: 221–32.
4 Li QL, Ito K, Sakakura C *et al*. Causal relationship between the loss of RUNX3 expression and gastric cancer. *Cell* 2002; **109**: 113–24.
5 Waki T, Tamura G, Sato M, Terashima M, Nishizuka S, Motoyama T. Promoter methylation status of DAP-kinase and RUNX3 genes in neoplastic and non-neoplastic gastric epithelia. *Cancer Sci* 2003; **94**: 360–4.
6 Kim TY, Lee HJ, Hwang KS *et al*. Methylation of RUNX3 in various types of human cancers and premalignant stages of gastric carcinoma. *Laboratory Invest* 2004; **84**: 479–84.
7 Oshimo Y, Oue N, Mitani Y *et al*. Frequent loss of RUNX3 expression by promoter hypermethylation in gastric carcinoma. *Pathobiology* 2004; **71**: 137–43.
8 Ku JL, Kang SB, Shin YK *et al*. Promoter hypermethylation downregulates *RUNX3* gene expression in colorectal cancer cell lines. *Oncogene* 2004; **23**: 6736–42.
9 Homma N, Tamura G, Honda T *et al*. Spreading of methylation within RUNX3 CpG islands in gastric cancer. *Cancer Sci* 2006; **97**: 51–6.
10 Wada M, Yazumi S, Takaishi S *et al*. Frequent loss of *RUNX3* gene expression in human bile duct and pancreatic cancer cell lines. *Oncogene* 2004; **23**: 2401–7.
11 Li QL, Kim HR, Kim WJ *et al*. Transcriptional silencing of the *RUNX3* gene by CpG hypermethylation is associated with lung cancer. *Biochem Biophys Res Commun* 2004; **314**: 223–8.
12 Park WS, Cho YG, Kim CJ *et al*. Hypermethylation of the *RUNX3* gene in hepatocellular carcinoma. *Exp Mol Med* 2005; **37**: 276–81.
13 Mori T, Nomoto S, Koshikawa K *et al*. Decreased expression and frequent allelic inactivation of the *RUNX3* gene at 1p36 in human hepatocellular carcinoma. *Liver Int* 2005; **25**: 380–8.
14 Xiao WH, Liu WW. Hemizygous deletion and hypermethylation of *RUNX3* gene in hepatocellular carcinoma. *World J Gastroenterol* 2004; **10**: 376–80.
15 Yamamura Y, Lee WL, Inoue K, Ida H, Ito Y. RUNX3 cooperates with Foxo3A to induce apoptosis in gastric cancer cells. *J Biol Chem* 2006; **281**: 5267–76.
16 Gossen M, Bujard H. Tight control of gene expression in mammalian cells by tetracycline-responsive promoters. *Proc Natl Acad Sci USA* 1992; **89**: 5547–51.
17 Gossen M, Freundlieb S, Bender G, Muller G, Hillen W, Bujard H. Transcriptional activation by tetracyclines in mammalian cells. *Science* 1995; **268**: 1766–9.
18 Kanegae Y, Makimura Y, Saito I. A simple and efficient method for purification of infectious recombinant adenovirus. *Jpn J Meth Sci Biol* 1994; **47**: 157–66.
19 Tatebe S, Matsuura T, Endo K *et al*. Adenoviral transduction efficiency partly correlates with expression levels of integrin αvβ5, but not αvβ3 in human gastric carcinoma cells. *Int J Mol Med* 1998; **2**: 61–4.
20 Osaki M, Moriyama M, Adachi K *et al*. Expression of RUNX3 protein in human gastric mucosa, intestinal metaplasia and carcinoma. *Eur J Clin Invest* 2004; **34**: 605–12.
21 Ito K, Liu Q, Salto-Tellez M *et al*. RUNX3, a novel tumor suppressor, is frequently inactivated in gastric cancer by protein mislocalization. *Cancer Res* 2005; **65**: 7743–50.
22 Wei D, Gong W, Oh SC *et al*. Loss of RUNX3 expression significantly affects the clinical outcome of gastric cancer patients and its restoration causes drastic suppression of tumor growth and metastasis. *Cancer Res* 2005; **65**: 4809–16.
23 Kischkel FC, Hellbardt S, Behrmann I *et al*. Cytotoxicity-dependent APO-1 (Fas/CD95)-associated proteins form a death-inducing signaling complex (DISC) with the receptor. *EMBO J* 1995; **14**: 5579–88.
24 Thorburn A. Death receptor-induced cell killing. *Cell Signal* 2004; **16**: 139–44.
25 Irmler M, Thome M, Hahne M *et al*. Inhibition of death receptor signals by cellular FLIP. *Nature* 1997; **388**: 190–5.
26 Scaffidi C, Fulda S, Srinivasan A *et al*. Two CD95 (Apo-1/Fas) signaling pathways. *EMBO J* 1998; **17**: 1675–87.
27 Nagata S. Apoptosis by death factor. *Cell* 1997; **88**: 355–65.
28 Tsujimoto Y, Shimizu S. Bcl-2 family: life-or-death switch. *FEBS Lett* 2000; **466**: 6–10.
29 Adachi K, Osaki M, Kase S, Takeda A, Ito H. Anti-Fas antibody-induced apoptosis and its signal transduction in human gastric carcinoma cell lines. *Int J Oncol* 2003; **23**: 713–19.
30 Cheung KJ, Li G. p33/ING1 enhances UVB-induced apoptosis in melanoma cells. *Exp Cell Res* 2002; **279**: 291–8.
31 Shiseki M, Nagashima M, Pedeux RM *et al*. P29ING4 and p28ING5 bind to p53 and p300, and enhance p53 activity. *Cancer Res* 2003; **63**: 2373–8.
32 Ozer A, Wu LC, Bruick RK. The candidate tumor suppressor ING4 represses activation of the hypoxia inducible factor (HIF). *Proc Natl Acad Sci USA* 2005; **102**: 7481–6.
33 Damdimopoulos AE, Miranda-Vizuete A, Pelto-Huikko M, Gustafsson JA, Spyrou G. Human mitochondrial thioredoxin. *J Biol Chem* 2002; **277**: 33 249–57.
34 Gupta S, Knowlton AA. HSP60, Bax, apoptosis and heart. *J Cell Mol Med* 2005; **9**: 51–8.
35 Chen M, Wang J. Initiator caspases in apoptosis signaling pathways. *Apoptosis* 2002; **7**: 313–19.
36 Sakahira H, Enari M, Nagata S. Cleavage of CAD inhibitor in CAD activation and DNA degradation during apoptosis. *Nature* 1998; **391**: 96–9.
37 Johnson JD, Han Z, Otani K *et al*. RyR2 and Calpain-10 delineate a novel apoptosis pathway in pancreatic islets. *J Biol Chem* 2004; **279**: 24 794–802.
38 Peng Z, Wei D, Wang L *et al*. RUNX3 inhibits the expression of vascular endothelial growth factor and reduces the angiogenesis, growth and metastasis of human gastric cancer. *Clin Cancer Res* 2006; **12**: 6386–94.
39 O'Reilly LA, Cullen L, Visvader J *et al*. The proapoptotic BH3-only protein bim is expressed in hematopoietic, epithelial, neuronal, and germ cells. *Am J Pathol* 2000; **157**: 449–61.

## Supplementary Material

The following supplementary material is available for this article:

**Table S1.**

This material is available as part of the online article from:

http://www.blackwell-synergy.com/doi/abs/10.1111/j.1349-7006.2008.00650.x

<http://www.blackwell-synergy.com/doi/abs/10.1111/j.1349-7006.2008.00650.x>

(This link will take you to the article abstract).

Please note: Blackwell Publishing are not responsible for the content or functionality of any supplementary materials supplied by the authors. Any queries (other than missing material) should be directed to the corresponding author for the article.



doi: 10.1111/j.1349-7006.2007.00650.x